PHYSICAL REVIEW B VOLUME 47, NUMBER 9 1 MARCH 1993-I

$1/N$ expansion and spin correlations in constrained wave functions

Maxim Raykin*
Physics Department, Boston University, Boston, Massachusetts 02215

Assa Auerbach†
Physics Department, Technion, Haifa 32000, Israel
and Physics Department, Boston University, Boston, Massachusetts 02215
(Received 25 August 1992)

We develop a large-N expansion for Gutzwiller projected spin states. We consider valence-bond singlets, constructed by Schwinger bosons or fermions, which are variational ground states for quantum antiferromagnets. This expansion is simpler than the familiar expansions of the quantum Heisenberg model, and thus more instructive. The diagrammatic rules of this expansion allow us to prove certain identities to all orders in $1/N$. We derive the on-site spin-fluctuations sum rule for arbitrary N. We calculate the correlations of the one-dimensional valence-bond solid states and the Gutzwiller projected Fermi gas up to order $1/N$. For the boson case, we are surprised to find that the mean-field, the order-$1/N$, and the exact correlations are simply proportional. For the fermion case, the $1/N$ correction enhances the zone-edge singularity. The comparison of our leading-order terms to known results for $N = 2$ enhances our understanding of large-N approximations in general.

I. INTRODUCTION

The use of large-N approximations to treat strongly interacting quantum systems has been very extensive in the last decade. The approach has originated in particle physics, but has found many applications in condensed matter systems. Some notable examples are the SU(N) quantum Heisenberg model,[1,2] the (closely related) nonlinear σ or CP^{N-1} models,[3,4] the Anderson and Kondo (Coqblin-Schrieffer) models,[5,6] and the two-band Hubbard model for cuprate superconductors.[7]

Generally speaking, the parameter N labels an internal SU(N) symmetry at each lattice site. In most cases, the large-N approximation has been applied to treat spin Hamiltonians, where the symmetry is SU(2), and N is therefore not a truly large parameter. Here lies its primary weakness, since in most cases the $N > 2$ models are not physically realizable. Nevertheless, the $1/N$ expansion provides an easy method for obtaining simple mean-field theories. These have been found to be either surprisingly successful, or completely wrong depending on the system. For example, the Schwinger boson mean-field theory works well for the quantum Heisenberg model, except for the half-odd integer antiferromagnet in one dimension.[1,2] The latter is better described by a fermion large-N approximation. It is important to investigate the conditions which allow certain large-N generalizations to yield a "better" mean-field theory for a particular N=2 system.

In contrast to spin wave expansions about a broken symmetry state, the large-N approach can describe both ordered and disordered phases. At $N = \infty$, the generating functional is dominated by its saddle point, which is a noninteracting mean-field theory with few variational parameters. The variational equations and the leading-order correlations are in many cases analytically tractable.

The corrections to the mean-field theory are given by Feynman diagrams, where the "interactions" are mediated by random-phase approximation (RPA) matrix propagators. It is hard in most cases to compute these diagrams even to first order in $1/N$, which is why they have been determined only in a few select cases.[5,6]

In this paper we shall start by deriving a new and simplified version of the large-N expansion suitable for evaluating spin correlations in constrained variational wavefunctions. These states have been used as trial ground states for various antiferromagnetic Heisenberg models. The exact calculation of their correlations is not feasible in most cases. In one dimension, two cases which have been solved analytically are the valence bonds solids (VBS), and the Gutzwiller-projected Fermi gas (GPFG). We shall make use of these exact solutions in this paper.

It is our primary purpose to study the properties of the $1/N$ expansion by using the constrained states as toy problems. Their $1/N$ expansion differs from that of, e.g., Ref. 1 in two respects: (i) Here, the generating functional has no time dependence and Matsubara sums and (ii) there is only one fluctuating field per site, the constraint field λ, and no Hubbard-Stratonovich fields. Thus, we study the "pure" effects of the constraints, without the interactions effects of the quartic Hamiltonian. These features simplify the evaluation of $1/N$ corrections considerably.

This paper is organized as follows. Section II introduces the valence bonds states. Section III introduces the Gutzwiller-projected Fermi gas states. Section IV defines the generating functional of the spin correlation

functions for both bosons and fermions states in a unified notation. Section V derives the $1/N$ expansion of the correlation functions and describes the diagrammatic rules. Section VI applies the diagrammatic rules to prove three identities to all orders in $1/N$: the absence of charge fluctuations, the sum rule for on-site spin fluctuations and the absence of zero momentum correlations. Section VII describes the results of the mean field and $1/N$ order spin correlations for the one dimensional VBS and GPFG states. *The most surprising result is that for the VBS states of integer spin, the mean field, $\mathcal{O}(1/N)$ correction, and the exact result for N=2 are simply proportional.* Section VIII summarizes what we have learned from our approach in the context of large-N approximations in general. It also lists some conjectures and open questions, which emerge from this study. Appendixes A, B, and C fill in some technical details which have been used to derive certain equations in the text.

II. SCHWINGER BOSONS VALENCE BONDS STATES

Schwinger bosons describe spin operators in a rotationally invariant formulation. The standard SU(2) spin operators are given by two commuting bosons a, b at each site as follows:

$$\begin{aligned} S_i^z &= \tfrac{1}{2}(a_i^\dagger a_i - b_i^\dagger b_i), \\ S_i^+ &= a_i^\dagger b_i, \\ S_i^- &= b_i^\dagger a_i. \end{aligned} \tag{2.1}$$

The spin size s is determined by projecting the states with the Gutzwiller operator $\mathcal{P}_s$ (Ref. 8) onto the subspace which obeys the local constraints at all sites

$$a_i^\dagger a_i + b_i^\dagger b_i = n_{ai} + n_{bi} = 2s\ . \tag{2.2}$$

A Schwinger boson mean field wave function is defined as

$$|\hat{u}\rangle = \exp\left[\frac{1}{2}\sum_{ij} u_{ij}(a_i^\dagger b_j^\dagger - b_i^\dagger a_j^\dagger)\right]|0\rangle, \tag{2.3}$$

where $u_{ij} = -u_{ji}$ are either determined by some mean-field Hamiltonian, or are taken as free variational parameters. It is easy to verify that due to the invariance of the forms $a_i^\dagger b_j^\dagger - b_i^\dagger a_j^\dagger$ under global spin rotations, $|\hat{u}\rangle$ is a total singlet. If we restrict u_{ij} to be *bipartite*, i.e., to connect only between two distinct sublattices, say A and B, then we can redefine the operators on sublattice B by sending

$$a_j \to -b_j, \quad b_j \to a_j, \quad j \in B, \tag{2.4}$$

and for $i \in A$, $j \in B$, $u_{ji} \to -u_{ji}$ and $u_{ij} \to u_{ij}$, so that $\hat{u}$ transforms into a symmetric matrix. Under (2.4) the mean-field wave function transforms into

$$|\hat{u}\rangle \to \exp\left[\frac{1}{2}\sum_{ij} u_{ij}(a_i^\dagger a_j^\dagger + b_i^\dagger b_j^\dagger)\right]|0\rangle. \tag{2.5}$$

Equations (2.2)–(2.5) can be generalized to SU(N) representations using N flavors of Schwinger bosons a_{im}, $m = 0, \ldots, N$. In order to construct symmetric forms in the mean-field wave function we again restrict ourselves to bipartite lattices, and define the SU(N) generalization $S_{imm'}$ of spin operators (2.2) as

$$S_{imm'} \equiv \begin{cases} a_{im}^\dagger a_{im'}, & i \in A, \\ -a_{im'}^\dagger a_{im}, & i \in B, \end{cases} \tag{2.6}$$

where we have generalized the SU(2) sublattice rotation (2.4) to SU(N).

The local constraints generalize to

$$\sum_{m=1}^{N} n_{im} \equiv n_i = Ns. \tag{2.7}$$

Ns is an integer, where s is a generalized "spin size."

The SU(N) generalization of our mean field wave function (2.5) is

$$|\hat{u}\rangle = \exp\left[\frac{1}{2}\sum_{ij} u_{ij}\sum_{m=1}^{N} a_{im}^\dagger a_{jm}^\dagger\right]|0\rangle. \tag{2.8}$$

We list some essential properties of these states in Appendix A.

It is easy to show that for any m, m', and bond (i_a, j_b) we use the definitions (2.6) and find that

$$\begin{aligned} \left[\sum_i S_{imm'}, \sum_{\mu=1}^{N} a_{i_a\mu}^\dagger a_{j_b\mu}^\dagger\right] &= 0, \\ \sum_i S_{imm'}|\hat{u}\rangle &= 0. \end{aligned} \tag{2.9}$$

Relations (2.9) show that $|\hat{u}\rangle$ is globally SU(N) invariant, and is therefore a *singlet of total spin.*

We shall restrict ourselves to translationally invariant states, which in Fourier representation are given by

$$|\hat{u}\rangle = \exp\left[\frac{1}{2}\sum_{\mathbf{k}\in \mathrm{BZ}} u_{\mathbf{k}}\sum_{m=1}^{N} a_{\mathbf{k}m}^\dagger a_{-\mathbf{k}m}^\dagger\right]|0\rangle, \tag{2.10}$$

where BZ is the first Brillouin zone, $u_{\mathbf{k}} = \sum_j e^{i\mathbf{k}j}u_{0j}$, $a_{\mathbf{k}m}^\dagger = \mathcal{N}^{-\frac{1}{2}}\sum_j e^{i\mathbf{k}j}a_{jm}^\dagger$, and $\mathcal{N}$ is the number of lattice sites. We also define $S_{\mathbf{k}mm'} = \sum_j e^{i\mathbf{k}j}S_{jmm'}$.

A. The Gutzwiller projection

The mean-field states (2.8) and (2.10) includes different spin sizes at each site. In order to construct a bona fide state of spins s, we must project out all other spin sizes using the Gutzwiller projector

$$|\hat{u}\rangle_s = \mathcal{P}_s|\hat{u}\rangle \tag{2.11}$$

which enforces the constraints (2.7). By expanding the exponential in (2.8) and applying the Gutzwiller projection we obtain

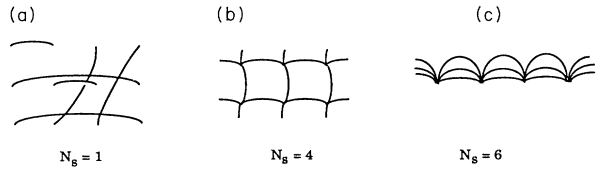

FIG. 1. Graphical representation of valence bonds configurations, which contribute to (a) resonating valence bonds states (RVB) on the square lattice. (b) Valence bonds solid on the square lattice. (c) Valence bonds solid on the chain.

$$|\hat{u}\rangle_s = \mathcal{P}_s \frac{1}{\nu_b!}\left(\frac{1}{2}\sum_{ij} u_{ij}\sum_{m=1}^{N} a_{im}^\dagger a_{jm}^\dagger\right)^{\nu_b}|0\rangle$$
$$= \frac{1}{\nu_b!}\sum_{\alpha}\prod_{(ij)\in C_\alpha} u_{ij}\left(\sum_{m=1}^{N} a_{im}^\dagger a_{jm}^\dagger\right)|0\rangle, \quad (2.12)$$

where $\nu_b = \frac{1}{2}\mathcal{N}Ns$ is the total number of bonds in the projected state and C_α labels the different configurations of ν_b bonds on the lattice, where exactly Ns bonds emanate from every site. In Fig. 1 we depict several configurations for various $\{u_{ij}\}$ and values of Ns. $|\hat{u}\rangle_s$, which is a sum over such configurations, is called a "valence bonds state."

Since all $S_{imm'}$ commute with the constraint, $|\hat{u}\rangle_s$ is also rotationally invariant and a total singlet. If all the bond parameters are non-negative, $u_{ij} \geq 0$, the wave function (2.12) satisfies the Marshall sign criterion.[9] We recall that the ground state of any bipartite Heisenberg antiferromagnet must be a total singlet and obey Marshall's theorem.

The correlation function in the Gutzwiller projected state is defined as

$$S^{mm'}(i,j) = \langle S_{imm'} S_{jm'm}\rangle \quad (2.13)$$

and its Fourier transform is

$$S^{mm'}(\mathbf{k}) = \sum_j S^{mm'}(0,j)\exp(i\mathbf{k}\cdot\mathbf{j})$$
$$= \frac{1}{\mathcal{N}}\langle S_{-\mathbf{k}mm'} S_{\mathbf{k}m'm}\rangle, \quad (2.14)$$

where for any operator $\mathcal{O}$ we denote

$$\langle\mathcal{O}\rangle \equiv \langle\hat{u}|\mathcal{P}_s\mathcal{O}\mathcal{P}_s|\hat{u}\rangle/\langle\hat{u}|\mathcal{P}_s|\hat{u}\rangle. \quad (2.15)$$

1. *Resonating valence bonds ($s = \frac{1}{2}$)*

Several special cases have received particular attention in the literature. For $N = 2$, $s = \frac{1}{2}$ and nearest neighbors $u_{\langle ij\rangle}$, $|\hat{u}\rangle_s$ is a superposition of all *dimer configurations*. In one dimension there are only two such (Majumdar-Ghosh) configurations,[10] which have an exponentially small overlap for large lattices. The spin correlation in one dimer state vanishes beyond the nearest-neighbor range. In two and higher dimensions, $s = \frac{1}{2}$ states are sums over many valence bonds configurations, which were denoted as "resonating valence bonds" (RVB) by Anderson.[11] One configuration in the square lattice RVB state is depicted in Fig. 1(a). The RVB state was proposed by Anderson[11] and others as trial ground states for frustrated quantum antiferromagnets and high-T_c superconductors. The number of dimer configurations grows exponentially with $\mathcal{N}$, and the overlap between different configurations is finite. The computation of the spin correlations in the dimer and longer range RVB state was carried out numerically by Liang, Doucot, and Anderson[12] using bipartite bonds of various range. They found that the RVB states with $u_{ij} \sim 1/r_{ij}^\alpha$ have long-range order for $\alpha \leq 5$.

2. *Valence bonds solids, integer s*

Affleck, Kennedy, Lieb, and Tasaki[13] (AKLT) found a class of extended SU(2) Heisenberg models for which the exact ground states are valence bond solid (VBS) states, given for SU(N) by

$$|\Psi^{\mathrm{VBS}}\rangle_s = \prod_{\langle ij\rangle}\left(\sum_{m=1}^{N} a_{im}^\dagger a_{jm}^\dagger\right)^{M}|0\rangle,$$
$$M = Ns/z, \quad (2.16)$$

where $\langle ij\rangle$ denotes nearest-neighbor bonds and z is the lattice coordination number. The condition that M must be an integer restricts the size of the spin and lattice for which such states can be defined [see Figs. 1(b) and 1(c)]. For example, the SU(2) model in one dimension allows $s = 1, 2, 3\ldots$. On the square lattice, only even spins $s = 2, 4, 6\ldots$ are allowed. The correlation function $S^{+-}(i,j) \equiv \langle\Psi^{\mathrm{VBS}}|S_i^+ S_j^-|\Psi^{\mathrm{VBS}}\rangle/\langle\Psi^{\mathrm{VBS}}|\Psi^{\mathrm{VBS}}\rangle$ for one dimension has been calculated for all s by Arovas, Auerbach, and Haldane[14] (AAH) to be

$$S^{+-}(i,j) = (-1)^{j-i}\frac{2(s+1)^2}{3}\exp\left[-\kappa_s|j-i|\right] - \delta_{ij}\frac{2(s+1)}{3},$$
$$\kappa_s = \ln(1+2/s), \quad (2.17)$$
$$S^{+-}(k) = \frac{2}{3}(s+1)\frac{1-\cos(k)}{1+\cos(k)+\frac{2}{s(s+2)}}.$$

The real-space correlations decay as a pure exponential, with $1/\kappa_s$ as the correlation length. $|\Psi^{\mathrm{VBS}}\rangle$ is a "spin liquid" ground state of the kind that was predicted by Haldane[15] using the large-s, nonlinear σ model analysis of the Heisenberg antiferromagnet. AAH also found a Haldane gap[15] in its single-mode excitation spectrum. The correlations of VBS states on higher dimensional lattices are those of a classical logarithmic Heisenberg model, at temperature $T = z/s$. This implies that for large enough s, the VB states in three dimensions have long-range Néel order. The calculation of Eq. (2.17) was performed in the SU(2) coherent states basis. The generalization of this calculation to $N > 2$ has not yet been

achieved. In the following we shall apply the large-N expansion to this problem.

It may be verified that the one-dimensional Schwinger boson state $|\hat{u}^{\rm VBS}\rangle_s$ with

$$u_{ij}^{\rm VBS} = \delta_{\langle ij\rangle}\ ,\quad u_k^{\rm VBS} = 2\cos(k)\ , \tag{2.18}$$

is dominated by the VBS state in the limit of infinite lattice size $\mathcal{N}$:

$$(M!)^{\frac{1}{2}\mathcal{N}z}\,|\hat{u}^{\rm VBS}\rangle_s = |\Psi^{\rm VBS}\rangle_s + |\Psi'\rangle, \tag{2.19}$$

where $\langle\Psi'|\Psi'\rangle \sim c^{-\mathcal{N}}$ for some $c > 1$. The exponentially small corrections are of non uniform valence bonds configurations, where some bonds have higher powers of $a^\dagger a^\dagger$ than others. Consequently, we expect that in the thermodynamic limit $\mathcal{N} \to \infty$ the spin correlation function in the state $|\hat{u}^{\rm VBS}\rangle_s$ is given also by (2.17).

III. GUTZWILLER-PROJECTED FERMI GAS

In this section we introduce another important family of variational states using fermions rather than Schwinger bosons, to represent the SU(N) spin operators

$$S_{imm'} \equiv a_{im}^\dagger a_{im'}\ ,\qquad a_{im}a_{jm'}^\dagger + a_{jm'}^\dagger a_{im} = \delta_{ij}\delta_{mm'}. \tag{3.1}$$

The local constraint on the fermion occupation is

$$\sum_{m=1}^{N} n_{im} \equiv n_i = Ns, \tag{3.2}$$

where Ns is an integer, which by the Pauli principle must be less than or equal to N. Using the fermion operators one can construct a global SU(N) singlet by the following state:

$$|\hat{u}\rangle_s = \mathcal{P}_s \prod_{|\mathbf{k}|\le k_F} \left(u_{\mathbf{k}} \prod_{m=1}^{N} a_{\mathbf{k}m}^\dagger \right) |0\rangle, \tag{3.3}$$

where k_F is the Fermi momentum which is chosen to include Ns states per site in the Fermi volume. $\mathcal{P}_s$ Gutzwiller projects onto the subspace which satisfies the constraint (3.2). $u_{\mathbf{k}}$ are variational parameters.

It is possible to write (3.3) in an exponential form as follows:

$$|\hat{u}\rangle_s = \mathcal{P}_s\ \exp\left[\frac{1}{2}\sum_{\mathbf{k}} u_{\mathbf{k}}\theta\left(k_F - |\mathbf{k}|\right)\ \sum_m a_{\mathbf{k}m}^\dagger a_{-\mathbf{k}m}^\dagger\right]|0\rangle, \tag{3.4}$$

where $u_{\mathbf{k}} = -u_{-\mathbf{k}}$. In real space (3.4) are analogous to the Schwinger boson states, defined in (2.11) and (2.8), where $u_{ij} = \mathcal{N}^{-1}\sum_{|\mathbf{k}|\le k_F} u_{\mathbf{k}} e^{i\mathbf{k}(i-j)}$, $u_{ji} = -u_{ij}$. A well-known case is the Gutzwiller-projected Fermi gas for $s = \frac{1}{2}$ (i.e., a half-filled Brillouin zone),

$$|\Psi^{\rm GPFG}\rangle = \mathcal{P}_{\frac{1}{2}}\ \exp\left[\frac{1}{2}\sum_{\mathbf{k}} {\rm sgn}(\mathbf{k})\theta\left(k_F - |\mathbf{k}|\right)\ \sum_m a_{\mathbf{k}m}^\dagger a_{-\mathbf{k}m}^\dagger\right]|0\rangle. \tag{3.5}$$

In real space $|\Psi^{\rm GPFG}\rangle$ contains long-range bonds u_{ij}, $|i-j| >> 1$. Since the bonds are not bipartite, it does not satisfy the Marshall sign criterion. This state is deduced from the mean-field theory of Baskaran, Zou, and Anderson[16] for the Heisenberg antiferromagnet. In one dimension, $|\Psi^{\rm GPFG}\rangle$ for SU(2) was found to be the exact ground state of the Haldane-Shastry Hamiltonian,[17] whose interactions fall off as the second inverse power of distance. This state has correlations, similar to that of the ground state of the nearest neighbor Heisenberg model. Haldane has also shown that the Haldane-Shastry Hamiltonian and the nearest-neighbor Heisenberg model share similar gapless excitation spectra.[17]

Gebhard and Vollhardt[18] have calculated the correlation function of one-dimensional $|\Psi^{\rm GPFG}\rangle$ for N=2:[19]

$$S^{+-}(k) = -\frac{1}{2}\ln\left(1 - \frac{|k|}{\pi}\right)\ , \tag{3.6}$$

which in real space decay asymptotically as a power law

$$S^{+-}(i,j) = \frac{{\rm Si}[\pi(j-i)]}{2\pi}\ \frac{(-1)^{(j-i)}}{j-i}, \tag{3.7}$$

where ${\rm Si}(x)$ is the sine integral function.

IV. CORRELATIONS AND THE GENERATING FUNCTIONAL

The spin correlations of $|\hat{u}\rangle_s$ can be derived from a generating functional. The generating functionals for the valence bonds states (2.11) and the Gutzwiller-projected Fermi gas states (3.4) are formally very similar, and given by

$$Z[j] = \left\langle\ \exp\left[\sum_{imm'} \eta_i j_{imm'} a_{im}^\dagger a_{im'}\right]\right\rangle, \tag{4.1}$$

where a_{im} are either bosons or fermions, $j_{imm'}$ are the source currents, $\eta_i = 1$ for fermions and for bosons

$$\eta_i = \begin{cases} 1, & i \in A \\ -1, & i \in B, \end{cases} \tag{4.2}$$

which takes care of the sublattice rotation of the SU(N) spins (2.6). The functional derivatives of Z determine the spin correlation functions. It is sufficient to use symmetric source matrices $j_{imm'} = j_{im'm}$. Hence, $j_{imm'}$ and $j_{im'm}$ *are not to be considered as independent*, but should be varied simultaneously when differentiating $Z[j]$.

The following relations can be directly verified from (4.1)

$$\eta_i \frac{\delta \ln Z}{\delta j_{imm'}}\bigg|_{j=0} = \delta_{mm'}\langle n_{im}\rangle = \delta_{mm'} s, \tag{4.3}$$

which is a direct consequence of the SU(N) symmetry in (2.8) and the constraint (2.7). The two-point spin correlation function Eq. (2.13) is given by

$$S^{mm'}(i,j) = \frac{1}{2-\delta_{mm'}} Z^{-1} \frac{\delta^2 Z}{\delta j_{imm'}\delta j_{jmm'}}\bigg|_{j=0}. \tag{4.4}$$

Additional terms generated by the differentiation in (4.4) must vanish, since

$$\langle S_{im\neq m'} S_{jm\neq m'}\rangle = 0. \tag{4.5}$$

Equation (4.5) follows from the rotational invariance of the wave function. It is easy to verify that $S_{im\neq m'}|\hat{u}\rangle_s$ and $S_{jm'\neq m}|\hat{u}\rangle_s$ are eigenstates of the operator $\sum_i (S_{imm} - S_{im'm'})$ with eigenvalues $+2$ and -2, respectively. Therefore these two states are orthogonal and (4.5) follows.

For $m \neq m'$, the correlation function $S^{m\neq m'}(i,j)$ is an SU(N) generalization of the usual SU(2) spin correlation function $S^{+-}(i,j) = \langle S_i^+ S_j^-\rangle$. In rotationally invariant states this function is related to the correlations of the other SU(2) spin components by

$$S^{m\neq m'}(i,j) = 2\langle S_i^z S_j^z\rangle = \tfrac{2}{3}\langle \mathbf{S}_i \cdot \mathbf{S}_j\rangle. \tag{4.6}$$

The evaluations of Z and $S^{mm'}(i,j)$ of Eqs. (4.1) and (4.4) are complicated because of the Gutzwiller projector. If it were absent, we could easily calculate Z as a matrix element of an exponential bilinear operator as done in Appendix A. In order to proceed, we must choose a convenient representation for the projector. The projector can be represented as a limit of a strongly interacting density matrix,

$$\mathcal{P}_s = \lim_{\epsilon\to 0} \exp\left[-\frac{1}{2N\epsilon^2}\sum_i (n_i - Ns)^2\right]. \tag{4.7}$$

Keeping ϵ finite will help to control infrared divergences in subsequent diagrammatic calculations. The matrix elements of (4.7) are hard to evaluate in its present form. Using an auxiliary constraint variable λ_i at every site, we transform (4.1) to an integral

$$\mathcal{P}_s = \lim_{\epsilon\to 0}\int_{-\infty}^{\infty} \mathcal{D}\lambda \exp\left[\sum_i\left(-\frac{N\epsilon^2}{2}\lambda_i^2 + i\lambda_i(n_i - Ns)\right)\right], \tag{4.8}$$

$$\mathcal{D}\lambda \equiv \prod_i \left(\epsilon\sqrt{\frac{N}{2\pi}} d\lambda_i\right).$$

Now we can write the generating functional as

$$Z[j] = \lim_{\epsilon\to 0}\int \mathcal{D}\lambda\, \langle\hat{u}|\exp\left[\mathbf{a}^\dagger(i\hat{\lambda}+\hat{j})\mathbf{a}\right]|\hat{u}\rangle \times e^{-iNs\sum_i\lambda_i - \frac{N\epsilon^2}{2}\sum_i\lambda_i^2}, \tag{4.9}$$

where we denote the matrices

$$\hat{\lambda} = \lambda_i\delta_{ii'}\delta_{mm'}, \quad \hat{j} = \eta_i j_{imm'}\delta_{ii'}. \tag{4.10}$$

In (4.9) we have used the commutation of the spins with the density operator,

$$\left[a_{im}^\dagger a_{im'}, n_{i'}\right] = 0 \tag{4.11}$$

to combine the exponentials of the source terms and the projector. Now we use Appendix A, to evaluate (4.9) as

$$Z[j] = \lim_{\epsilon\to 0}\int \mathcal{D}\lambda \exp\left(N\mathcal{S}[\lambda, j]\right), \tag{4.12}$$

$$\mathcal{S}[\lambda,j] = -\frac{\zeta}{2N}\mathrm{Tr}_{im}\ln\left(1-\zeta\hat{u}^\dagger e^{i\hat{\lambda}+\hat{j}}\hat{u}e^{i\hat{\lambda}+\hat{j}}\right) - is\sum_i\lambda_i - \frac{\epsilon^2}{2}\sum_i\lambda_i^2,$$

where $\zeta = +1$ (-1) for bosons (fermions) and $\hat{u}^\dagger$ is the Hermitian conjugate of the matrix $\hat{u}$.

The correlation function is given by Eq. (4.4):

$$S^{mm'}(1,2) = \frac{1}{2-\delta_{mm'}}\lim_{\epsilon\to 0} Z^{-1}\int \mathcal{D}\lambda \left(N\frac{\delta^2\mathcal{S}[\lambda,j]}{\delta j_{1mm'}\delta j_{2mm'}} + N^2\frac{\delta\mathcal{S}[\lambda,j]}{\delta j_{1mm'}}\frac{\delta\mathcal{S}[\lambda,j]}{\delta j_{2mm'}}\right)\bigg|_{j=0} \exp\left(N\mathcal{S}[\lambda]\right), \tag{4.13}$$

where $\mathcal{S}[\lambda] = \mathcal{S}[\lambda,j]\big|_{j=0}$.

V. THE DIAGRAMMATIC EXPANSION OF $Z(j)$

The multidimensional integration over $\mathcal{D}\lambda$ is equivalent to the difficult combinatorical problem of evaluating the correlations in the valence bonds state, e.g., (2.12). This is clearly seen by expanding the action in powers of $e^{i\lambda_i}$ and integrating with the weights $e^{-iNs\lambda_i}$. The integrals reduce to products of δ functions, which select the terms with Ns powers of u_{ij} for any given site i. Summation over these terms is very cumbersome in general.

In (4.12) and (4.13) the parameter N was scaled out of the action $\mathcal{S}$. We shall evaluate the λ integrals by a saddle-point expansion which is controlled by the largeness of N. The functional $\mathcal{S}[\lambda]$ is expanded as a Taylor

series about its minimum $\bar{\lambda}$; the coefficients of expansion are independent of N. Since the wave function is translationally invariant we shall search in the space of *uniform* saddle points $\bar{\lambda}_i = \bar{\lambda}$. $\bar{\lambda}$ is found by requiring that the linear variations vanish. We define $e^{i\bar{\lambda}} = \bar{u}$. The saddle-point or "mean-field" equation is

$$\frac{1}{i}\frac{\delta \mathcal{S}[\lambda]}{\delta \lambda_j}\bigg|_{\bar{\lambda}} = [\bar{u}^2\hat{u}^\dagger\hat{u}(1-\zeta\bar{u}^2\hat{u}^\dagger\hat{u})^{-1}]_{jj} - s = 0, \qquad (5.1)$$

which determines $\bar{u}[\hat{u}, S]$. We see that (5.1) implies that $\bar{u}$ is real, i.e., the integration paths of the variables λ_i have to be analytically continued to cross the imaginary axis at $\bar{\lambda} = -i\ln(\bar{u})$. The term $[\,]_{jj}$ in (5.1) is the average number of particles of every flavor in the (unconstrained) state $|\bar{u}\hat{u}\rangle$ (see Appendix A). Thus, the mean-field equation yields that the constraint is satisfied on the average. If we define the unprojected state using $\bar{u}\hat{u}$ instead of $\hat{u}$, the mean-field equation (5.1) would be satisfied with $\bar{\lambda} = 0$. Hence we shall use that convention for $\hat{u}$ and set $\bar{\lambda} = 0$.

We now expand $\mathcal{S}$, in powers of λ to obtain

$$\mathcal{S}[\lambda] = \mathcal{S}^{(0)} - \frac{1}{2}\sum_{ij}\mathcal{S}^{(2)}_{ij}\lambda_i\lambda_j + \mathcal{S}^{\rm int}, \qquad (5.2)$$

where $\mathcal{S}^{\rm int}$ includes only third- and higher-order terms:

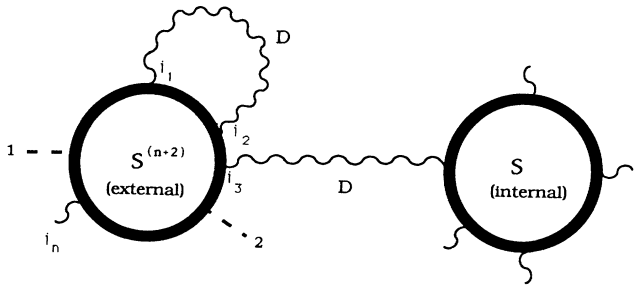

FIG. 2. Diagrammatic representation of the $1/N$ expansion for the correlation function $S(1,2)$. Thick circles denote loops, wiggly lines are λ propagators, and dashed lines are external currents.

$$\mathcal{S}^{\rm int} = \sum_{n=3}^{\infty}\frac{i^n}{n!}\mathcal{S}^{(n)}_{i_1,\ldots,i_n}\lambda_{i_1}\cdots\lambda_{i_n}. \qquad (5.3)$$

$\mathcal{S}^{(n)}$ here depend parametrically on $\bar{u}$. Diagrammatically they are depicted as thick circles with n λ vertices denoted by wiggly lines (see Fig. 2). Later we shall obtain explicit expressions for $\mathcal{S}^{(n)}$ in form of *loops* constructed of Greens functions.

We also expand the preexponential functions in (4.13)

$$\frac{\delta \mathcal{S}[\lambda, j]}{\delta j_{1mm'}}\bigg|_{j=0} = \frac{\delta_{mm'}\eta_1}{N}\left(\sum_{n=1}^{\infty}\frac{i^n}{n!}\mathcal{S}^{(n+1)}_{1,i_1,\ldots,i_n}\lambda_{i_1}\cdots\lambda_{i_n} + s\right) = \frac{\delta_{mm'}\eta_1}{N}\sum_{n=0}^{\infty}\frac{i^n}{n!}\mathcal{S}^{(n+1)}_{1,i_1,\ldots,i_n}\lambda_{i_1}\cdots\lambda_{i_n},$$

$$\frac{1}{2-\delta_{mm'}}\frac{\delta^2\mathcal{S}[\lambda, j]}{\delta j_{1mm'}\delta j_{2mm'}}\bigg|_{j=0} = \frac{\eta_1\eta_2}{N}\sum_{n=0}^{\infty}\frac{i^n}{n!}\mathcal{S}^{(n+2)}_{1,2,i_1,\ldots,i_n}\lambda_{i_1}\cdots\lambda_{i_n}, \qquad (5.4)$$

where sums over repeated indices are assumed and we denoted $\mathcal{S}^{(1)}_1 = s$. Here we use (4.12) to relate the derivatives with respect to λ to those with respect to j. Diagrammatically, we denote the current vertices (at points $1, 2$) by dashed lines as shown in Fig. 2.

The correlations functions can be evaluated by inserting the expansions (5.2) and (5.4) into (4.13)

$$S^{mm'}(1,2) = \eta_1\eta_2\left[S^I(1,2) + \delta_{mm'}S^{II}(1,2)\right], \qquad (5.5)$$

where

$$S^I(1,2) = \lim_{\epsilon\to 0} Z^{-1}\int \mathcal{D}\lambda\left(\sum_{n=0}^{\infty}\frac{i^n}{n!}\mathcal{S}^{(n+2)}_{1,2,i_1,\ldots,i_n}\lambda_{i_1}\cdots\lambda_{i_n}\right) \times\sum_{L=0}^{\infty}\frac{N^L}{L!}\left(\sum_{n=3}^{\infty}\frac{i^n}{n!}\mathcal{S}^{(n)}_{i_1,\ldots,i_n}\lambda_{i_1}\cdots\lambda_{i_n}\right)^L \exp\left(-\frac{N}{2}\mathcal{S}^{(2)}_{kl}\lambda_k\lambda_l\right),$$

$$S^{II}(1,2) = \lim_{\epsilon\to 0} Z^{-1}\int \mathcal{D}\lambda\left(\sum_{n=0}^{\infty}\frac{i^n}{n!}\mathcal{S}^{(n+1)}_{1,i_1,\ldots,i_n}\lambda_{i_1}\cdots\lambda_{i_n}\right)\left(\sum_{n=0}^{\infty}\frac{i^n}{n!}\mathcal{S}^{(n+1)}_{2,i_1,\ldots,i_n}\lambda_{i_1}\cdots\lambda_{i_n}\right) \times\sum_{L=0}^{\infty}\frac{N^L}{L!}\left(\sum_{n=3}^{\infty}\frac{i^n}{n!}\mathcal{S}^{(n)}_{i_1,\ldots,i_n}\lambda_{i_1}\cdots\lambda_{i_n}\right)^L \exp\left(-\frac{N}{2}\mathcal{S}^{(2)}_{kl}\lambda_k\lambda_l\right). \qquad (5.6)$$

We disregard the contribution of the constant $N\mathcal{S}^{(0)}$ in the action.

The integrals in (5.6) are sums of multidimensional Gaussian integrals. The Gaussian integrations contract all λ fields in pairs $\overbrace{\lambda_k\lambda_l}$ bringing down a propagator for each pair given by

$$D_{kl} = \overbrace{\lambda_k\lambda_l} = -\frac{1}{N}\left(S^{(2)}\right)^{-1}_{kl}, \tag{5.7}$$

where the minus sign is due to the factor of i, which accompanies every λ field. The propagator (5.7) is depicted as a wavy line connecting two λ vertices in Fig. 2. One has to sum over all λ contractions. The disconnected parts of the diagrams serve to cancel the factor of Z^{-1}, leaving us with the diagrams which are connected to one or the other current vertices (a linked-cluster theorem). Thus calculating any particular diagram involves multiplying loops $\mathcal{S}^{(n)}$ and propagators D, and summing over internal lattice points. There are *internal* loops, created by powers of $\mathcal{S}^{\rm int}$, and *external* loops, coming from an expansion of the preexponential functions (5.4). Internal loops must have at least three λ vertices; external loops have current vertices and might also have arbitrary (including zero) number of λ vertices. The order of any particular diagram is given by

$$\left(\frac{1}{N}\right)^{P-L}, \tag{5.8}$$

where L is the number of internal loops [or the power L of the sums in (5.6)], and P is the number of propagators [half the number of λ fields in (5.6)]. After grouping all the diagrams at each order in 1/N we obtain the series

$$S^{mm'}(1,2) = \sum_{p=0}^{\infty} N^{-p} S^{mm'\,(p)}(1,2). \tag{5.9}$$

Similar rules govern the calculation of higher correlation functions. One has to sum over all possible ways of distributing the current vertices on the external loops. Within each loop the m, m' indices of the external currents must be equal to the indices of other external currents, to allow nonzero values of the trace.

VI. IDENTITIES TO ALL ORDERS

The diagrammatic expansion of the $1/N$ *series has special structure which allow us to obtain exact identities to all orders in* $1/N$. A key feature is that the propagator D of the constraint field λ is none other than the inverse of the square part of the action $\mathcal{S}^{(2)}$. As a result we shall show that the local constraints are exactly enforced to each order in the expansion, i.e., there are no contributions to charge fluctuations when all terms of the same order are considered. In addition we shall prove a sum rule for the on site spin fluctuations for arbitrary N and the absence of zero momentum off-diagonal spin correlations.

A. Absence of charge fluctuations

Here we shall demonstrate that the constraint is imposed at each order in $1/N$. In other words, due to the Gutzwiller projection the density fluctuations vanish identically after all diagrams of a given order are summed, yielding

$$\langle n_1 \mathcal{A}\rangle = Ns\,\langle \mathcal{A}\rangle \tag{6.1}$$

for an arbitrary operator $\mathcal{A}$. It is instructive to see how (6.1) is derived by the diagrammatic expansion. A current of n_1 belongs to some external loop $\mathcal{S}^{(n+1)}$, $n \geq 0$. Let us first consider all the contributions with $n \geq 1$. We define a *"tail"* of a diagram as the combination of a propagator attached in series to a loop $S^{(2)}$ which has the operator n_1 on its other vertex. All diagrams can be separated into two classes: ones with a tail, and ones without a tail. It is easy to identify for each diagram without a tail say $R(n_1, \mathcal{A})$, a counterterm $\bar{R}(n_1, \mathcal{A})$ by attaching a tail to the n_1 vertex (See Fig. 3). By (5.7) the two are of the same order p (they have the same number of loops minus propagators) and they cancel precisely

$$\begin{aligned}\bar{R}(n_1, \mathcal{A}) &= N \sum_{kl} \mathcal{S}^{(2)}_{1,k} D_{kl} R(n_l, \mathcal{A}) \\ &= -R(n_1, \mathcal{A}).\end{aligned} \tag{6.2}$$

Thus, at any order p, the counterterms cancel the connected charge fluctuation diagrams one by one. The only terms in the expansion of $\langle n_1 \mathcal{A}\rangle$ which survive are the disconnected contributions with n_1 on the loop $\mathcal{S}^{(1)}$. An important property of the diagram rules is the absence of the counterterm to the $\mathcal{S}^{(1)}$ loop. Such counterterm would involve an internal loop $\mathcal{S}^{(1)}$, which is not allowed by the rules of our expansion. Thus (6.1) follows from $\mathcal{S}^{(1)} = s$. Q.E.D.

B. Sum rule for the on-site spin fluctuations

First we shall show that for SU(N) invariant states there is a relation between two types of correlation functions: diagonal S^{mm} and off-diagonal $S^{m\neq m'}$. Both functions do not depend on the particular values of m, m' since the wave functions are SU(N) symmetric. Due to the $\delta_{mm'}$ coefficient in (5.5), $S^{m\neq m'}$ is equal to S^I. Let S^{mm}_c be the connected part of the diagonal correlation function. Any diagram which contributes to the off-diagonal correlations also appears in S^{mm}_c, i.e.,

$$\text{if} \quad R^\alpha \in S^{m\neq m'}, \quad \text{then} \quad R^\alpha \in S^{mm}_c. \tag{6.3}$$

However, in S^{mm}_c its contribution is partially canceled by

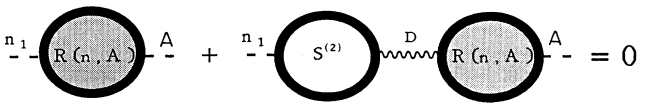

FIG. 3. Diagrammatic representation of cancellation of charge fluctuations by counterterms, Eq. (6.2).

the counterterms, which are given by tails insertion. It may be seen that the sum of any diagram $R^\alpha \in S^{m\neq m'}$ and its counterterms, obtained by all possible ways of insertion of tails, is equal to $(1-1/N)R^\alpha$.

In addition to diagrams of the type R^α and their counterterms, yet another contribution to S_c^{mm} is given by the diagrams R^β, which have the two current vertices on different loops $\mathcal{S}^{(n_1+1)}$ and $\mathcal{S}^{(n_2+1)}$, $n_{1,2}\geq 2$, and by their counterterms $\bar{R}^\beta$. But the diagrams R^β must exactly cancel with their counterterms! This is verified by adding a tail to one of the loops and seeing that the counterterm is of the same order in $1/N$ due to the additional m summation for the loop which became an internal loop. This proves that all the diagrams which do not cancel are of the type R^α and the following important identity holds:

$$S_c^{mm}(i,j) = \left(1-\frac{1}{N}\right) S^{m\neq m'}(i,j). \tag{6.4}$$

Now we can calculate the onsite spin fluctuations. For SU(2) we are familiar with the "spin square" operator $\mathbf{S}^2$, which when projected to the s sector yields a diagonal matrix of elements $s(s+1)$. For larger N, its natural generalization is

$$\begin{aligned}\mathbf{S}_i^2 &\equiv \mathcal{P}_{Ns}\sum_{mm'} S_{imm'}S_{im'm}\\ &= \mathcal{P}_{Ns}\sum_{mm'}\left(n_{im'}(1+\zeta n_{im})-\zeta\delta_{mm'}n_{im'}\right)\\ &= \left(N^2 s(1+\zeta s)-\zeta N\right)\ \mathcal{P}_{Ns},\end{aligned} \tag{6.5}$$

where in the fermion case we made use of equality $n_{im}^2 = n_{im}$ ($\zeta=-1$). On the other hand, using (6.4) we can write the on-site fluctuations as

$$\begin{aligned}\langle \mathbf{S}_i^2\rangle &= \sum_{m\neq m'} S^{m\neq m'}(i,i)+\sum_m [S_c^{mm}(i,i)+\langle n_{im}\rangle^2]\\ &= \left[N(N-1)+N\left(1-\frac{1}{N}\right)\right] S^{m\neq m'}(i,i)+Ns^2.\end{aligned} \tag{6.6}$$

Using (6.5) we find the desired identity

$$S^{m\neq m'}(i,i) = \frac{N}{N+\zeta}\, s(1+\zeta s). \tag{6.7}$$

For SU(2) this formula reduces to the known values

$$\langle S_i^+ S_i^-\rangle = \begin{cases}\frac{2}{3}s(s+1) & \text{Schwinger bosons,}\\ \frac{1}{2} & \text{fermions } (s=\frac{1}{2}).\end{cases} \tag{6.8}$$

In translationally invariant cases (6.7) gives a sum rule, which is useful for checking the diagrammatic calculations at each order of 1/N separately. In momentum space, the diagrams of order $(1/N)^p$ must obey

$$\mathcal{N}^{-1}\sum_{\mathbf{k}} S^{m\neq m'(p)}(\mathbf{k}) = \left(\frac{1}{N}\right)^p (-\zeta)^p s(1+\zeta s), \qquad p=0,1,2,\ldots. \tag{6.9}$$

C. Absence of zero-momentum correlations

The last identity is a consequence of the singlet nature of the wavefunction which implies that $S_{\mathbf{k}=0\, m\neq m'}|\hat{u}\rangle_s = 0$. By using Eq. (2.14) we obtain from that

$$S^{m\neq m'}(\mathbf{k}=0) = 0\,, \tag{6.10}$$

which holds of course at each and every order in the $1/N$ series.

VII. CALCULATIONS OF LEADING ORDERS

In this section we calculate the spin correlation functions $S^{m\neq m'}$ using the $1/N$ expansion. We start with an explicit evaluation of the loops $\mathcal{S}^{(n)}$ and propagator D. In the cases of interest $\hat{u}$ is Hermitian. It is useful to define the following *Greens functions*

$$\hat{u}_\pm = \zeta^{1/2}\bar{u}\hat{u}\left(\pm 1-\zeta^{1/2}\bar{u}\hat{u}\right)^{-1}. \tag{7.1}$$

We also introduce the matrix $\Lambda = \delta_{ij}(e^{i\lambda_j}-1)$ and express the action (4.12) as

$$\begin{aligned}\mathcal{S}[\lambda] &= \mathcal{S}^{(0)} - \frac{\zeta}{2}\sum_{\gamma=\pm}\mathrm{Tr}\,\ln(1-\hat{u}_\gamma\Lambda)\\ &\quad -is\sum_i\lambda_i - \frac{\epsilon^2}{2}\sum_i\lambda_i^2,\\ \mathcal{S}^{(0)} &= -\frac{\zeta}{2}\sum_{\gamma=\pm}\mathrm{Tr}\,\ln(1-\gamma\zeta^{1/2}\bar{u}\hat{u}).\end{aligned} \tag{7.2}$$

$\mathcal{S}^{(0)}$ is a constant which we shall disregard.

Expanding the logarithm in (7.2) and using (5.1) to cancel the linear term we obtain

$$\mathcal{S}[\lambda] = \frac{\zeta}{2}\sum_{\gamma,\,n=1}^{\infty}{}'\frac{1}{n}\mathrm{Tr}\,(\hat{u}_\gamma\Lambda)^n - \frac{\epsilon^2}{2}\sum_j\lambda_j^2, \tag{7.3}$$

where $\sum'$ denotes that terms linear in λ are excluded. By equating terms of the same order in λ in Eqs. (5.2) and (7.3) we can relate the loops $\mathcal{S}^{(n)}$, $n\geq 2$ to traces over Greens functions u_γ. Diagrammatically, we denote the Greens functions by thin sold lines. A closed loop of Greens functions denotes a trace over lattice and γ indices. For a n λ vertices $\mathcal{S}^{(n)}$, there are contributions from diagrams with $1\leq m\leq n$ Greens functions, since the function Λ yields all powers of λ fields at the same point. Due to Eq. (7.4) below, the loop $\mathcal{S}^{(1)}$ may be denoted diagrammatically in the same manner—as a closed loop of one Greens function with one vertex.

The translational invariance of $\hat{u}$ makes it easier to work in the momentum representation. The linear action, or the mean-field equation (5.1), is explicitly given by

$$\frac{\zeta}{2}(\hat{u}_+ + \hat{u}_-)_{jj} = \frac{1}{\mathcal{N}}\sum_{\mathbf{k}}\bar{u}^2\frac{|u_{\mathbf{k}}|^2}{1-\zeta\bar{u}^2|u_{\mathbf{k}}|^2} = s. \tag{7.4}$$

The quadratic action in (5.2) is given by

$$\mathcal{S}^{(2)}_{ij} = \frac{\zeta}{2}\sum_{\gamma}(u_{\gamma ij}u_{\gamma ji} + \delta_{ij}u_{\gamma ii}) + \delta_{ij}\epsilon^2 = \frac{\zeta}{2}\sum_{\gamma}u_{\gamma ij}u_{\gamma ji} + \delta_{ij}s + \delta_{ij}\epsilon^2,$$

$$\mathcal{S}^{(2)}(\mathbf{q}) = \frac{\zeta}{2\mathcal{N}}\sum_{\mathbf{k}}\sum_{\gamma=\pm}u_{\gamma\mathbf{k}}\,u_{\gamma\mathbf{k}+\mathbf{q}} + s + \epsilon^2 = \frac{1}{2\mathcal{N}}\sum_{\mathbf{k}}\sum_{\gamma=\pm 1}\frac{\bar{u}^2 u_{\mathbf{k}}\,u_{\mathbf{k}+\mathbf{q}}}{(\gamma-\zeta^{1/2}\bar{u}u_{\mathbf{k}})\,(\gamma-\zeta^{1/2}\bar{u}u_{\mathbf{k}+\mathbf{q}})} + s + \epsilon^2, \tag{7.5}$$

and the propagator is

$$D(\mathbf{q}) = -\,[N\mathcal{S}^{(2)}(\mathbf{q})]^{-1}. \tag{7.6}$$

An important property of this expansion is that the lowest order (mean field) correlation function $S^{m\neq m'\,(0)}(\mathbf{q})$ is simply related to the quadratic part of the action:

$$S^{m\neq m'\,(0)}(i,j) = \eta_i\eta_j\mathcal{S}^{(2)}(i,j),$$
$$S^{m\neq m'\,(0)}(\mathbf{q}) = \begin{cases}\mathcal{S}^{(2)}(\mathbf{q}+\boldsymbol{\pi}), & \text{Schwinger bosons},\\ \mathcal{S}^{(2)}(\mathbf{q}), & \text{fermions},\end{cases} \tag{7.7}$$

where $\boldsymbol{\pi} = (\pi, \pi, \ldots)$ for a cubic lattice. The diagrams for $S^{m\neq m'\,(0)}(\mathbf{q})$ are shown in Fig. 4. At this point we note that $D(\mathbf{q})$ is singular for $\epsilon \to 0$ since $S^{m\neq m'\,(0)}(\mathbf{q}=0)$ vanishes by (6.10). This causes diagrams which involve one or more propagators to diverge as $1/\epsilon$. A check on the correctness of the calculation is that these "infrared" divergences must exactly cancel between different diagrams to yield a finite result for $\lim_{\epsilon\to 0} S^{(p)}(1,2)$ for each order p separately. We shall come back to this point in our summary.

The $1/N$ corrections for $S^{m\neq m'}(\mathbf{k})$ are given by the diagrams of Fig. 5. Solid lines represent factors of $u_\gamma(k)$. Each vertex conserves momentum, and indices $\gamma = +,-$ of the solid lines. We must sum over internal momenta and γ. Diagrams with external currents 1,2 at the same point denote an overall factor of δ_{12}. Due to the cancellation mechanism described in Sec. VI A, the third and fourth diagrams in the bottom row of Fig. 5 cancel against the fifth diagram. Thus by the same mechanism, there is complete cancellation between the last four diagrams in the second row. We shall describe the calculations of the remaining diagrams for the Scwhinger boson and fermion cases separately, and defer technical details to Appendixes B and C.

A. Valence bonds solid correlations

The mean-field equation Eq. (7.4) for the valence bonds solid state (2.18) is

$$\int_{-\pi}^{\pi}\frac{dk}{2\pi}\,\frac{4\bar{u}^2\cos^2(k)}{1-4\bar{u}^2\cos^2(k)} = s, \tag{7.8}$$

whose solution is

$$\bar{u}(s) = \frac{\sqrt{s(s+2)}}{2(s+1)}\,. \tag{7.9}$$

By (7.7) and (7.5) we obtain

$$S^{m\neq m'(0)}(k) = -2\bar{u}^2\sum_{\gamma=\pm 1}\int_{-\pi}^{\pi}\frac{dq}{2\pi}\,\frac{\cos(q)\cos(k+q)}{[\gamma-2\bar{u}\cos(q)][\gamma+2\bar{u}\cos(k+q)]} + s. \tag{7.10}$$

The integral is evaluated by introducing a new variable $z = e^{iq}$ which transforms the integration over q into an integration along a unit circle $|z| = 1$ in the complex z plane. Using (7.9) yields

$$S^{m\neq m'(0)}(k) = (s+1)\,\frac{1-\cos(k)}{1+\cos(k)+\frac{2}{s(s+2)}}. \tag{7.11}$$

This result is very surprising, since it is just proportional to the exact result for $N = 2$ as found by Ref. 14 and given in Eq. (2.17). The factor $\frac{2}{3}$ between (2.17) and the mean-field result (7.11) is consistent with the factor $N/(N+1)$ between the mean-field on-site fluctuations and the exact sum rule, Eq. (6.7). This suggests that

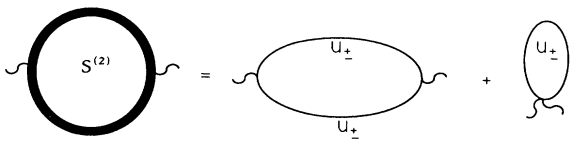

FIG. 4. The diagrams contributing to the loop $\mathcal{S}^{(2)}$. $u_\pm$ are mean-field Greens functions, defined in Eq. (7.1).

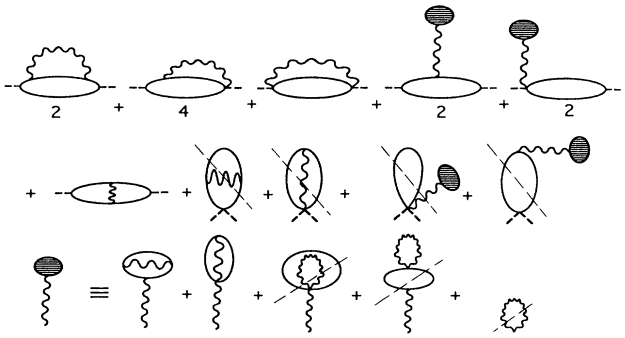

FIG. 5. The $1/N$ corrections to $S^{m\neq m'}(\mathbf{k})$. See discussion after Eq. (7.7).

perhaps the exact N dependence of $S^{m\neq m'}(k)$ is given by this simple multiplicative factor. Fortunately, we are able to calculate the $\mathcal{O}(1/N)$ corrections and check this proposition at least to the next leading order in $1/N$. This calculation is described by the diagrams of Fig. 5, which involve exchanges of one or two propagators D. The sum of all diagrams was evaluated analytically using the symbolic manipulation program MATHEMATICA.[20] The result, derived in Appendix B, is

$$S^{m\neq m'(1)}(k) = -\frac{1}{N} S^{m\neq m'(0)}(k). \tag{7.12}$$

This result confirms the above hypothesis, but is far from obvious. In fact, the separate $1/N$ diagrams have infrared divergences of order ϵ^{-1} due to the diverging propagators at momentum π. In addition, the separate diagrams have different correlation lengths than the mean-field function, but these effects somehow cancel by summing *all* the terms of order $1/N$, leaving us with Eq. (7.12). It is highly tempting to conjecture that the same relation holds to all orders, i.e., that

$$S^{m\neq m'(p)}(k) = \left(-\frac{1}{N}\right)^p S^{m\neq m'(0)}(k) \quad (?) \tag{7.13}$$

which will sum up to the simple relation

$$S^{m\neq m'}(k) = \frac{N}{N+1} S^{m\neq m'(0)}(k) \quad (?). \tag{7.14}$$

For $N = 2$ we have already seen that this conjecture is correct. But, as we shall discuss in Sec. VIII, *the underlying reason for this relation is still a mystery.*

B. Fermions GPFG correlations

The mean-field equation (7.4) for the one-dimensional GPFG state $|\Psi^{\mathrm{GPFG}}\rangle$ (3.5) is given by the integral

$$\frac{\bar{u}^2}{1+\bar{u}^2} \int_{-\pi}^{\pi} \frac{dk}{2\pi} \theta(k_F - |k|) - s = 0, \tag{7.15}$$

with $k_F = \pi/2$ and $s = \frac{1}{2}$. Equation (7.15) yields

$$\bar{u}(s) = \frac{1}{\sqrt{\frac{k_F}{\pi s} - 1}} \tag{7.16}$$

which implies that for $k_F \to \pi/2$ and $s = \frac{1}{2}$, $\bar{u} \to \infty$. To enable us to calculate the correlations for the GPFG, we keep $\bar{u}$ finite by holding a Fermi level k_F a little above $\pi/2$. We shall take the limit $k_F \to \pi/2$ only at the end of our calculations. This divergence simplifies the calculations considerably, because Eq. (7.1) yields a simple limit

$$\lim_{k_F \to \frac{\pi}{2}} u_{\pm}(q) = -\theta\left(\frac{\pi}{2} - |q|\right). \tag{7.17}$$

The lowest-order correlation function is evaluated using (7.7), (7.5), and (7.17)

$$\begin{aligned} \lim_{k_F \to \frac{\pi}{2}} S^{m\neq m'(0)}(k) &= \frac{1}{2} - \int_{-\pi}^{\pi} \frac{dq}{2\pi} \theta\left(\frac{\pi}{2} - |q|\right) \theta\left(\frac{\pi}{2} - |k+q|\right) \\ &= \frac{|k|}{2\pi}. \end{aligned} \tag{7.18}$$

When comparing (7.18) to Gebhard and Vollhardt's result, Eq. (3.6), we find that the two expressions agree very well in the small k limit, where they vanish with the same linear coefficient, but they deviate at larger k as shown in Fig. 6. Equation (3.6) diverges logarithmically near $k = \pi$, while the mean-field result (7.18) has merely a discontinuity in its derivative. This translates to a difference in the asymptotic power-law decay in real space, between $1/|i-j|$ of Eq. (3.7) and $1/|i-j|^2$ of (7.18). There is a factor of $N/(N-1) = 2$ between their sum rules as required by Eq. (6.7).

In Appendix C we calculate the $1/N$ diagrams for the GPFG state. We obtain the result:

$$S^{m\neq m'(1)}(k) = \frac{1}{N}\left[\frac{|k|}{\pi} + \left(1 - \frac{|k|}{\pi}\right) \ln\left(1 - \frac{|k|}{\pi}\right)\right]. \tag{7.19}$$

In Fig. 6 we compare the functions $S^{m\neq m'(0)}(k)$, $S^{m\neq m'(0)}(k) + S^{m\neq m'(1)}(k)$ and the exact result Eq. (3.6) for N=2. We see that the $1/N$ correction improves the mean-field approximation considerably near the zone boundary, where its derivative diverges logarithmically. In real space we obtain for separations $r = |j-i|$,

$$S^{m\neq m'(1)}(r) = \frac{(-1)^r}{N\pi^2 r^2} [\gamma + \ln(\pi r) - Ci(\pi r)] \tag{7.20}$$

where $\gamma = 0.577\cdots$ is the Euler constant and $Ci(x) = -\int_x^{\infty} dt \cos(t)/t$ vanishes for large x. In (7.20) we find that the $1/N$ correction enhances the long-distance correlations from r^{-2} to $r^{-2}\ln(r)$.

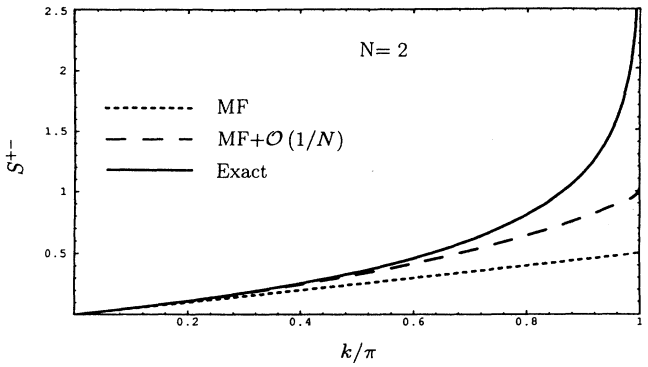

FIG. 6. The N=2 spin correlations of the Guztwiller-projected Fermi gas in one dimension. The exact result (solid line, from Ref. 18) diverges at $k = \pi$. The mean-field (MF, short dashes) result has discontinuous derivatives at $k = 0, \pi$, while the sum up to order $1/N$ (long dashed line) has a diverging derivative at $k = \pi$ [see Eq. (7.19)].

VIII. SUMMARY AND DISCUSSION

In this paper we have introduced a large-N expansion for the correlation functions of Gutzwiller-projected states. We have discovered several properties and sum rules which hold to all orders in $1/N$. By explicitly calculating the mean field and $1/N$ corrections for particular Schwinger boson and fermion states, we can check the validity of this approach against exact results for $N = 2$. We shall conclude by discussing what we believe we have learned from our results, and what still needs to be illuminated by further investigations and insight.

A. What we understand

(1) The effects of the Gutzwiller projector can be expanded systematically in terms of $1/N$ diagrams. Each diagram with L loops and P propagators is of order $(1/N)^{(P-L)}$. The loops and propagators are determined by the mean-field (saddle-point) equation.

(2) The local charge fluctuations are suppressed at each order by counterterms, which have the tail structure depicted in Fig. 3.

(3) For any N, the on-site spin fluctuations are given by

$$\langle S_{im\neq m'} S_{im'\neq m}\rangle = \frac{N}{N+\zeta} s(1+\zeta s), \tag{8.1}$$

where $\zeta = 1$ (-1) for bosons (fermions).

(4)Each diagram can diverge due to the divergence of the propagators [see discussion after Eq. (7.7)]. However, the sum of all diagrams of the $1/N$ order is finite. We conclude that in general, large-N expansions are prone to such intermediate divergences, due to the "hardness" of the constraints (or lack of "self-interaction" for the λ fields). The lesson to be learned is that *results which are based on any subset of diagrams, or on partial resummation schemes, are highly suspect.*

B. What we do not understand

(1) For the VBS states, the mean field, $\mathcal{O}(1/N)$ and the exact $N = 2$ correlations are simply proportional. We conjecture that the higher-order terms behave in the same manner, i.e.,

$$S^{m\neq m'}(k) = \frac{N}{N+1} S^{m\neq m'(0)}(k) \quad (?). \tag{8.2}$$

For Schwinger bosons, we know that this relation holds for the on-site sum rule (8.1), but its validity for all k is a surprise. We can recall however that similar surprises have been found in other large-N calculations, both with bosons and with fermions, where mean field results differ from the exact result by the factor $N/(N+\zeta)$. For example, the mean-field susceptibilities of the $s = \frac{1}{2}$ ferromagnet in one dimension, and antiferromagnet in two dimensions[1] (both for $N = 2$) are off by a factor of $\frac{2}{3} = N(N+1)$. Also, the Wilson ratios of the Kondo impurity model[5] and the $s = \frac{1}{2}$ Heisenberg antiferromagnetic chain[1] are $2 = N/(N-1)$. It would therefore be very useful to understand this relation in order to correct the mean-field approximation for other problems. The apparent simplicity of this correction factor may have its origin in some group theoretical relation between the saddle-point approximation and exact integrals over Haar measures.[21]

(2) The above discussion indicates that for these systems the $1/N$ expansion is not just an asymptotic series but a convergent, well-behaved expansion. On the other hand we are faced with the apparent failure of the boson large-N theory for the valence bonds solid at $s = \frac{1}{2}$ in one dimension. The $1/N$ series yields exponentially decaying correlations, while the correct state (the nearest-neighbor dimers state) has vanishing correlations beyond nearest-neighbor separations. We therefore strongly suspect that there is an essential singularity in the expansion of the form

$$\tfrac{1}{2}\left[1 + \exp(i2\pi N s)\right] \tag{8.3}$$

which cannot be obtained at any order in the expansion. Such a factor distinguishes between integer and half odd integer spins for $N = 2$. This is similar to the famous topological Berry's phase, or "θ term," of the continuous theory of half odd integer Heisenberg antiferromagnets in one dimension. This term must be added to the Schwinger boson mean field Lagrangian to obtain the correct ground state degeneracies.[2]

(3) We note that the Fermion large-N approximation is quite successful for the $s = \frac{1}{2}$ GPFG state in one dimension. The $1/N$ corrections enhance the long-distance correlations from r^{-2} to $r^{-2}\ln(r)$. It would be interesting to find out how the full $1/N$ series modifies the power law to r^{-1} for $N = 2$.

We recall that the fermion mean-field theory for the spin half Heisenberg chain[16] is successful in reproducing the Fermi-liquid features of the exact solution.[1] Here we have found another empirical evidence that the fermionic approach is better than the bosonic approach for $s = \frac{1}{2}$ antiferromagnets in one dimension. In two dimensions, the relative advantage of the fermionic versus bosonic large-N approach is not clear.

ACKNOWLEDGMENTS

This work has been supported by the National Science Foundation, NSF-DMR-9213884, and Grant No. 90-0041/1 from the U.S.-Israel Binational Science Foundation.

APPENDIX A: THE PROPERTIES OF MEAN-FIELD STATES

The major goal of this appendix is the derivation of Eq. (4.12). We will define here the mean-field states $|\hat{u}\rangle$ by

$$|\hat{u}\rangle = \exp\left[\frac{1}{2}\sum_{ij} u_{ij} a_i^\dagger a_j^\dagger\right]|0\rangle, \tag{A1}$$

where a_i are either bosons or fermions, satisfying the usual commutate relations

$$\begin{aligned} &a_i a_j^\dagger - \zeta a_j^\dagger a_i = \delta_{ij}, \\ &a_i a_j - \zeta a_j a_i = a_i^\dagger a_j^\dagger - \zeta a_j^\dagger a_i^\dagger = 0, \end{aligned} \tag{A2}$$

$\zeta = +1$ (-1) for bosons (fermions) and matrix $\hat{u}$ satisfies the symmetry condition $\hat{u}^T = \zeta\hat{u}$ $(u_{ij}^T = u_{ji})$. We have dropped the m indices for simplicity. The states $|\hat{u}\rangle$ have the following important properties:

(1) The overlap of mean-field states is given by

$$\langle\hat{u}|\hat{v}\rangle = \left[\det(1 - \zeta\hat{u}^\dagger\hat{v})\right]^{-\frac{\zeta}{2}}. \tag{A3}$$

(2) Let A be an arbitrary operator, the product of any number of creation and annihilation operators. Then the extended Wick's theorem holds: the normalized matrix element of A, $\langle\hat{u}|A|\hat{v}\rangle/\langle\hat{u}|\hat{v}\rangle$, is equal to the sum of all possible completly contracted products of creation and anihilation operators (with the usual sign for fermions), in which each contraction involves two operators. A contraction of d_1, d_2 is the normalized expectation value $\langle\hat{u}|d_1 d_2|\hat{v}\rangle/\langle\hat{u}|\hat{v}\rangle$.

(3) The contractions are given by

$$\begin{aligned} \frac{\langle\hat{u}|a_i a_j|\hat{v}\rangle}{\langle\hat{u}|\hat{v}\rangle} &= \zeta[\hat{v}(1 - \zeta\hat{u}^\dagger\hat{v})^{-1}]_{ij} \\ &= \left(\frac{\langle\hat{v}|a_j^\dagger a_i^\dagger|\hat{u}\rangle}{\langle\hat{v}|\hat{u}\rangle}\right)^*, \\ \frac{\langle\hat{u}|a_i^\dagger a_j|\hat{v}\rangle}{\langle\hat{u}|\hat{v}\rangle} &= [\hat{u}^\dagger\hat{v}(1 - \zeta\hat{u}^\dagger\hat{v})^{-1}]_{ij} \\ &= \zeta\frac{\langle\hat{u}|a_j a_i^\dagger|\hat{v}\rangle}{\langle\hat{u}|\hat{v}\rangle} - \zeta\delta_{ij}. \end{aligned} \tag{A4}$$

The proof of these properties may be found in Ref. 22 (see also Ref. 23).

Following Ref. 22 we will write the whole set of creation and annihilation operators as a $2\mathcal{N}$-dimensional vector ($\mathcal{N}$ is the lattice size):

$$\gamma \equiv \{\mathbf{a}, \mathbf{a}^\dagger\} \equiv \{a_1, \ldots, a_\mathcal{N}, a_1^\dagger, \ldots, a_\mathcal{N}^\dagger\} \tag{A5}$$

with commutation relations

$$\gamma_i\gamma_j - \zeta\gamma_j\gamma_i = \rho_{ij}, \tag{A6}$$

where ρ is the $2\mathcal{N} \times 2\mathcal{N}$ matrix

$$\rho = \begin{pmatrix} 0 & 1 \\ -\zeta & 0 \end{pmatrix}. \tag{A7}$$

We have $\rho^2 = -\zeta$, so $\rho^{-1} = -\zeta\rho$. Following Balian and Brezin[22] we define

$$\mathcal{J} = \exp\left[\frac{1}{2}\gamma R\gamma\right] \equiv \exp\left[\frac{1}{2}\sum_{i,j=1}^{2\mathcal{N}} \gamma_i R_{ij}\gamma_j\right], \tag{A8}$$

where the $2\mathcal{N}\times 2\mathcal{N}$ matrix R satisfies the symmetry condition $R^T = \zeta R$ (in this appendix we will call such matrices symmetric) and $2\mathcal{N} \times 2\mathcal{N}$ matrices

$$T \equiv \begin{pmatrix} T_{11} & T_{12} \\ T_{21} & T_{22} \end{pmatrix} = e^{\rho R}. \tag{A9}$$

It is shown in Ref. 22 that the matrices (A9) faithfully represent the second quantized operators (A8), i.e.,

$$\mathcal{J}(R_1)\mathcal{J}(R_2) = \mathcal{J}(R) \quad \Rightarrow \quad e^{\rho R_1}e^{\rho R_2} = e^{\rho R}. \tag{A10}$$

We will now prove the inverse statement,

$$e^{\rho R_1}e^{\rho R_2} = e^{\rho R} \quad \Rightarrow \quad \mathcal{J}(R_1)\mathcal{J}(R_2) = \mathcal{J}(R), \tag{A11}$$

that is to say, the representation of operators $\mathcal{J}$ by matrices T is isomorphic. To prove the (A11), we use the Baker-Campbell-Hausdorff formula, which gives[24]

$$e^{c_1}e^{c_2} = \exp\left(\sum_{n=1}^{\infty}\sum_{l_1,\ldots,l_n=1,2} \alpha_{l_1,\ldots,l_n}[c_{l_n}[c_{l_{n-1}}\cdots[c_{l_2}, c_{l_1}]\cdots]]\right), \tag{A12}$$

where we denoted $c_{1,2} = \frac{1}{2}\gamma R_{1,2}\gamma$ and $\alpha_{l_1,\ldots,l_n}$ are some constants, which we do not need to know explicitly. On the other hand, since $e^{\rho R_1}e^{\rho R_2} = e^{\rho R}$, the same formula gives

$$R = \rho^{-1}\sum_{n=1}^{\infty}\sum_{l_1,\ldots,l_n=1,2} \alpha_{l_1,\ldots,l_n}[\rho R_{l_n}[\rho R_{l_{n-1}}\cdots[\rho R_{l_2}, \rho R_{l_1}]\cdots]]. \tag{A13}$$

Correspondingly, (A11) will be proven, if one can show that

$$[c_{l_n}[c_{l_{n-1}}\cdots[c_{l_2}, c_{l_1}]\cdots]] = \tfrac{1}{2}\gamma\rho^{-1}[\rho R_{l_n}[\rho R_{l_{n-1}}\cdots[\rho R_{l_2}, \rho R_{l_1}]\cdots]]\gamma. \tag{A14}$$

Let us denote

$$A_n = \rho^{-1}[\rho R_{l_n}[\rho R_{l_{n-1}} \cdots [\rho R_{l_2}, \rho R_{l_1}] \cdots]], \quad \text{(A15)}$$

so that the right-hand side (RHS) of (A14) is equal to $\frac{1}{2}\gamma A_n \gamma$. We will first prove by induction, that A_n is symmetric, $A_n^T = \zeta A_n$. For $n = 1$ it is correct; then, for A_{n+1} we have

$$\begin{aligned} A_{n+1} &= \rho^{-1}[\rho R_{l_{n+1}}, \rho A_n] \\ &= R_{l_{n+1}} \rho A_n - A_n \rho R_{l_{n+1}}, \end{aligned} \quad \text{(A16)}$$

and since $R_{l_{n+1}}$ is symmetric and ρ is antisymmetric, $\rho^T = -\zeta\rho$, the symmetry of A_{n+1} follows from the symmetry of A_n.

Now we will prove by induction the relation (A14). For $n = 1$ it is trivially correct; then, if it is correct for n, we have for $n + 1$:

$$[c_{l_{n+1}}[c_{l_n} \cdots [c_{l_2}, c_{l_1}] \cdots]] = [\tfrac{1}{2}\gamma R_{l_{n+1}}\gamma, \tfrac{1}{2}\gamma A_n \gamma]. \quad \text{(A17)}$$

Using symmetry of $R_{l_{n+1}}$ and A_n and the commutation relation for γ (A6) it is straightforward to show that RHS of (A17) is equal to

$$\begin{aligned} &\tfrac{1}{2}\gamma\rho^{-1}[\rho R_{l_{n+1}}, \rho A_n]\gamma \\ &\quad = \tfrac{1}{2}\gamma\rho^{-1}[\rho R_{l_{n+1}}[\rho R_{l_n} \cdots [\rho R_{l_2}, \rho R_{l_1}] \cdots]]\gamma, \end{aligned} \quad \text{(A18)}$$

which completes the proof of (A11). Note that we have also shown that the product of two operators of the type (A8) is another operator of the same type, represented by the matrix R of (A13).

Now we shall use this "multiplication rule" to calculate (4.9). The expectation value is of the form

$$\begin{aligned} M &= \langle\hat{u}| \exp\left[\mathbf{a}^\dagger \hat{\eta} \mathbf{a}\right] |\hat{u}\rangle \\ &= \langle 0|\mathcal{J}_1 \exp\left[\mathbf{a}^\dagger \hat{\eta} \mathbf{a}\right] \mathcal{J}_2 |0\rangle, \end{aligned} \quad \text{(A19)}$$

where $\mathcal{J}_1 = \exp\left[\frac{1}{2}\mathbf{a}\hat{u}^\dagger \mathbf{a}\right]$ and $\mathcal{J}_2 = \exp\left[\frac{1}{2}\mathbf{a}^\dagger \hat{u} \mathbf{a}^\dagger\right]$ are operators of the type (A8) and $\hat{\eta}$ is $\mathcal{N} \times \mathcal{N}$ matrix. We can transform $\exp\left[\mathbf{a}^\dagger \hat{\eta} \mathbf{a}\right]$ also into the form (A8) by writing

$$\begin{aligned} \exp\left[\mathbf{a}^\dagger \hat{\eta} \mathbf{a}\right] &= \exp\left[-\frac{\zeta}{2}\mathrm{Tr}\,\hat{\eta}\right] \exp\left[\frac{1}{2}\gamma \begin{pmatrix} 0 & \zeta\hat{\eta}^T \\ \hat{\eta} & 0 \end{pmatrix} \gamma\right] \\ &\equiv \exp\left[-\frac{\zeta}{2}\mathrm{Tr}\,\hat{\eta}\right] \mathcal{J}_3, \end{aligned} \quad \text{(A20)}$$

where $\mathcal{J}_3$ is of the type (A8), so we have for M

$$\begin{aligned} M &= \exp\left[-\frac{\zeta}{2}\mathrm{Tr}\,\hat{\eta}\right] \langle 0|\mathcal{J}_1\mathcal{J}_3\mathcal{J}_2|0\rangle \\ &= \left[\det e^{\hat{\eta}}\right]^{-\frac{\zeta}{2}} \langle 0|\mathcal{J}_1\mathcal{J}_3\mathcal{J}_2|0\rangle. \end{aligned} \quad \text{(A21)}$$

The T matrices, corresponding to $\mathcal{J}_1$, $\mathcal{J}_2$, and $\mathcal{J}_3$ are

$$\begin{aligned} T_1 &= \exp\left[\begin{pmatrix} 0 & 1 \\ -\zeta & 0 \end{pmatrix}\begin{pmatrix} \hat{u}^\dagger & 0 \\ 0 & 0 \end{pmatrix}\right] = \begin{pmatrix} 1 & 0 \\ -\zeta\hat{u}^\dagger & 1 \end{pmatrix}, \\ T_2 &= \exp\left[\begin{pmatrix} 0 & 1 \\ -\zeta & 0 \end{pmatrix}\begin{pmatrix} 0 & 0 \\ 0 & \hat{u} \end{pmatrix}\right] = \begin{pmatrix} 1 & \hat{u} \\ 0 & 1 \end{pmatrix}, \\ T_3 &= \exp\left[\begin{pmatrix} 0 & 1 \\ -\zeta & 0 \end{pmatrix}\begin{pmatrix} 0 & \zeta\hat{\eta}^T \\ \hat{\eta} & 0 \end{pmatrix}\right] = \begin{pmatrix} e^{\hat{\eta}} & 0 \\ 0 & e^{-\hat{\eta}^T} \end{pmatrix}. \end{aligned} \quad \text{(A22)}$$

Thus, T, which corresponds to $\mathcal{J} = \mathcal{J}_1\mathcal{J}_3\mathcal{J}_2$, is

$$T = T_1T_3T_2 = \begin{pmatrix} e^{\hat{\eta}} & e^{\hat{\eta}}\,\hat{u} \\ -\zeta\,\hat{u}^\dagger e^{\hat{\eta}} & e^{-\hat{\eta}^T} - \zeta\,\hat{u}^\dagger e^{\hat{\eta}}\,\hat{u} \end{pmatrix}. \quad \text{(A23)}$$

It is shown in Ref. 22, that for every operator $\mathcal{J}$ (A8) and corresponding matrix T the following relation holds:

$$\langle 0|\mathcal{J}|0\rangle = [\det T_{22}]^{-\frac{\zeta}{2}}. \quad \text{(A24)}$$

Using Eqs. (A24), (A23), and (A21) we will obtain for the case of *symmetric* (in usual sense) $\hat{\eta}$, $\hat{\eta}^T = \hat{\eta}$, the final relation

$$\begin{aligned} \langle\hat{u}| \exp\left[\mathbf{a}^\dagger \hat{\eta} \mathbf{a}\right] |\hat{u}\rangle &= \left[\det\left(1 - \zeta\,\hat{u}^\dagger e^{\hat{\eta}}\,\hat{u} e^{\hat{\eta}}\right)\right]^{-\frac{\zeta}{2}} \\ &= \exp\left[-\frac{\zeta}{2}\mathrm{Tr}\ln\left(1 - \zeta\,\hat{u}^\dagger e^{\hat{\eta}}\,\hat{u} e^{\hat{\eta}}\right)\right], \end{aligned} \quad \text{(A25)}$$

which yields the expression (4.12) for the generating functional (4.9).

APPENDIX B: CALCULATION OF (7.12)

Here we explicitly calculate the $1/N$ order diagrams for the Schwinger boson case. The diagrams are depicted in Fig. 5. We use the integration variable $z = e^{ik}$ instead of the momentum k. For example, for the nearest-neighbor bonds problem $\hat{u}^{\mathrm{VBS}}$ of (2.18), we have

$$u^{\mathrm{VBS}}(z) = z + \frac{1}{z}. \quad \text{(B1)}$$

The conservation of momentum at every vertex is equivalent to the rule that the product of all z's entering a vertex is equal to unity. Each sum over k (Ref. 25) is replaced in the thermodynamic limit by a contour integration over z on the unit circle

$$\begin{aligned} \lim_{\mathcal{N}\to\infty} \mathcal{N}^{-1} \sum_k F_k &= \frac{1}{2\pi}\int_{-\pi}^{\pi} dk F_k \\ &\longrightarrow \frac{1}{2\pi i}\oint_{|z|=1} \frac{dz}{z} F(z) \\ &= \sum_i \mathrm{Res}\left[F(z_i)/z_i\right]. \end{aligned} \quad \text{(B2)}$$

For the quadratic part of the action (7.5) the integral is

$$\mathcal{S}^{(2)}(z) = \frac{1}{2}\sum_\gamma \frac{1}{2\pi i}\oint \frac{dz'}{z'} u_\gamma(z') u_\gamma(zz') + s + \epsilon^2, \quad \text{(B3)}$$

where

$$u_\pm(z) = \bar{u}u(z)\left[\pm 1 - \bar{u}u(z)\right]^{-1} \quad \text{(B4)}$$

and for the valence bond case $u(z)$ is given by (B1) and $\bar{u}$ by (7.9).

Since trigonometric integrands F_k are replaced by rational functions $F(z)$, it is easy to determine their poles z_i (including a pole at $z = 0$), and their residues at these poles. The sum over residues in (B3) yields

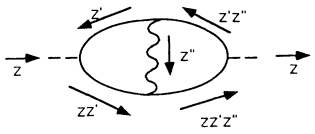

FIG. 7. Assignments of integration variables in Eq. (B7).

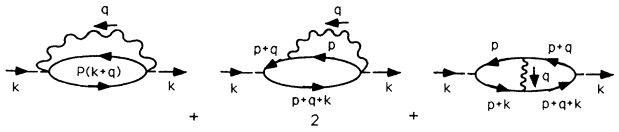

FIG. 8. Diagrams contributing to the correlations of the GPFG (Appendix C).

$$\mathcal{S}^{(2)}(z) = (s+1)\kappa\frac{(z+1)^2}{(z-\kappa)(1-z\kappa)} + \epsilon^2, \tag{B5}$$

where

$$\kappa = \frac{s}{s+2}\,. \tag{B6}$$

The propagator $D(z)$ is equal to $-\left(N\mathcal{S}^{(2)}(z)\right)^{-1}$. The diagrams are generated by the rules of Sec. III, and shown in Fig. 5. As an example, the integrations of the vertex diagram (see Fig. 7) are

$$\frac{1}{2}\sum_{\gamma}\frac{1}{(2\pi i)^2}\oint\frac{dz'}{z'}\oint\frac{dz''}{dz''}\,u_\gamma(z')\,u_\gamma(zz') \times u_\gamma(zz'z'')\,u_\gamma(z'z'')\,D(z'')\ . \tag{B7}$$

Each diagram in Fig. 5 diverges as $1/\epsilon$. However, the divergences cancel in the sum, and the overall 1/N result is finite for $\epsilon \to 0$. The simplicity of the residues method allowed us to use the symbolic manipulation program "MATHEMATICA"[20] to perform the integrations analytically on the computer. The program identifies the poles and residues of the rational functions. Intermediate expressions, especially for the diagram Fig. 7, involved up to hundreds of terms. Expanding these terms and finding common denominators became too cumbersome for manual calculations, and therefore automating this process was essential. The result of this calculation is given by Eq. (7.12).

APPENDIX C: CALCULATION OF (7.19)

Here we derive the order $1/N$ correlations of the Gutzwiller-projected Fermi gas state, Eq. (7.19). The quadratic part of the action is given by (7.18), so by (7.6), we have a diverging propagator at $k = 0$. We control this divergence by letting $k_F > \pi/2$. We denote

$$\frac{2k_F}{\pi} - 1 \equiv \frac{\delta}{2\pi} > 0\,. \tag{C1}$$

The role of δ is similar to that of ϵ – it regulates the divergence of the propagator. Thus we obtain

$$\mathcal{S}^{(2)}(k) = \frac{\delta + |k|}{2\pi}\,, \tag{C2}$$

so that

$$D(k) = -\frac{1}{N}\frac{2\pi}{\delta + |k|}\,. \tag{C3}$$

We first note that the last two diagrams of the top row in Fig. 5 cancel since they differ by one u_γ line, which yields a factor of -1. For the same reason, the sum of the first two diagrams is equal to twice the contribution of the second diagram. The remaining contributions to $\mathcal{S}^{m\neq m'(1)}(k)$ are depicted (including combinatorial factors) in Fig. 8. By reflection symmery we can restrict ourselves to $k > 0$.

The first diagram of Fig. 8 is given by

$$R_1(k) = \int_{-\pi}^{\pi} D(q)P(k+q)\frac{dq}{2\pi}, \tag{C4}$$

where $P(k)$ is the polarization bubble. By Fig. 4, for k in the first Brillouin zone

$$P(k) = \mathcal{S}^{(2)}(k) - s = \frac{|k|}{2\pi} - \frac{1}{2}\,, \tag{C5}$$

which yields for (C4)

$$R_1(k) = \frac{1}{N}\left[\left(1-\frac{k}{\pi}\right)\ln\frac{\pi-k}{\delta} - \frac{k}{\pi}\ln\frac{k}{\pi} + \frac{2k}{\pi} - 1\right]. \tag{C6}$$

The contribution of the second diagram of Fig. 8 is

$$2R_2(k) = 2\int_{-\pi}^{\pi}\frac{dq}{2\pi}D(q)\int_{-\pi}^{\pi}\frac{dp}{2\pi}\,\theta\left(\frac{\pi}{2} - |p|\right)\,\theta\left(\frac{\pi}{2} - |p+q|\right)\,\theta\left(\frac{\pi}{2} - |p+q+k|\right)\,. \tag{C7}$$

We denote the integral over p in (C7) as $(2\pi)^{-1}A(q)$, where

$$A(q) = \begin{cases} \pi + q & \text{if } -\pi \le q \le -k \\ \pi - k & \text{if } -k \le q \le 0 \\ (\pi - q - k)\,\theta\,(\pi - q - k) & \text{if } 0 \le q \le \pi \end{cases} \tag{C8}$$

which yields

$$2R_2(k) = \frac{1}{N}\left[-\frac{1}{\pi}\int_{-\pi}^{-k}\frac{\pi+q}{-q}dq - \frac{1}{\pi}\int_{-k}^{0}\frac{\pi-k}{\delta-q}dq - \frac{1}{\pi}\int_{0}^{\pi-k}\frac{\pi-q-k}{\delta+q}dq\right]. \tag{C9}$$

The last diagram of Fig. 8 is

$$R_3(k) = -\int_{-\pi}^{\pi}\frac{dq}{2\pi}D(q)\int_{-\pi}^{\pi}\frac{dp}{2\pi}\,\theta\left(\frac{\pi}{2}-|p|\right)\,\theta\left(\frac{\pi}{2}-|p+k|\right)\theta\left(\frac{\pi}{2}-|p+q|\right)\,\theta\left(\frac{\pi}{2}-|p+k+q|\right). \tag{C10}$$

The integral over p is equal to $(2\pi)^{-1}(\pi-k-|q|)\,\theta(\pi-k-|q|)$, so (C10) cancels the last term of (C9), while first two terms of (C9) yield

$$2R_2(k) + R_3(k) = \frac{1}{N}\left(\ln\frac{\delta}{\pi} - \frac{k}{\pi}\ln\frac{\delta}{k} + 1 - \frac{k}{\pi}\right). \tag{C11}$$

By adding (C11) and (C6) we obtain Eq. (7.19).

---

*Electronic address: raykin@buphy.bu.edu
†Electronic address: assa@phassa.technion.ac.il

[1]D. P. Arovas and A. Auerbach, Phys. Rev. B **38**, 316 (1988); A. Auerbach and D. P. Arovas, Phys. Rev. Lett. **61**, 617 (1988); J. Appl. Phys. **67**, 5734 (1990).
[2]N. Read and S. Sachdev, Nucl. Phys. B **316**, 609 (1989); Phys. Rev. Lett. **62**, 1694 (1989).
[3]A. D'Adda, M. Luscher, and P. Di Vecchia, Nucl. Phys. B **146**, 63 (1978); E. Witten, *ibid.* **149**, 285 (1979).
[4]For a review of the $1/N$ expansion in field theories, see, e.g., S. Coleman, *Aspects of Symmetry* (Cambridge University Press, Cambridge, England, 1985); and A. M. Polyakov, *Gauge Fields and Strings* (Harwood, New York, 1987).
[5]N. Read and D. M. Newns, J. Phys. C **16**, 3273 (1983); P. Coleman, Phys. Rev. B **35**, 3702 (1987).
[6]A. Auerbach and K. Levin, Phys. Rev. Lett. **57**, 877 (1986); A. J. Millis and P. A. Lee, Phys. Rev. B **35**, 3394 (1987).
[7]G. Kotliar, P. A. Lee, and N. Read, Physica C **153-155**, 538 (1988); J. H. Kim, K. Levin, and A. Auerbach, Phys. Rev. B **39**, 11 633 (1989).
[8]This generalizes the partial projector operator introduced by M. C. Gutzwiller, Phys. Rev. Lett. **10**, 159 (1963); Phys. Rev. **134**, A923 (1964); **137**, A1726 (1965).
[9]W. Marshall, Proc. R. Soc. London **A232**, 48 (1955); E. Lieb, T. Schultz, and D. Mattis, Ann. Phys. (N.Y.) **16**, 407 (1961).
[10]C. K. Majumdar and D. K. Ghosh, J. Math. Phys. **10**, 1388 (1969); **10**, 1399 (1969); C. K. Majumdar, J. Phys. C **3**, 911 (1970).
[11]P. W. Anderson, Science **235**, 1196 (1987).
[12]S. Liang, B. Doucot, and P. W. Anderson, Phys. Rev. Lett. **61**, 365 (1988).
[13]I. Affleck, T. Kennedy, E. H. Lieb, and H. Tasaki, Phys. Rev. Lett. **59**, 799 (1987); Commun. Math. Phys. **115**, 477 (1988).
[14]D. P. Arovas, A. Auerbach, and F. D. M. Haldane, Phys. Rev. Lett. **60**, 531 (1988).
[15]F. D. M. Haldane, Phys. Rev. Lett. **50**, 1153 (1983); Phys. Lett. **93A**, 464 (1983).
[16]G. Baskaran, Z. Zou, and P. W. Anderson, Solid State Commun. **63**, 973 (1987).
[17]F. D. M. Haldane, Phys. Rev. Lett. **60**, 635 (1988); B. S. Shastry, *ibid.* **60**, 639 (1988).
[18]F. Gebhard and D. Vollhardt, Phys. Rev. Lett. **59**, 1472 (1987).
[19]Note, that definition of spin operators in Ref. 18 is different from our equation (2.1) by a factor of 2, so we divided their spin correlation function by 4 to put it in agreement with our notations.
[20]S. Wolfram, *Mathematica: a System for Doing Mathematics by Computer*, 2nd ed. (Addison-Wesley, Redwood City, CA, 1991). The diagram integration program is available from the authors.
[21]We are grateful to Michael Stone for a discussion of some existing mathematical work on this subject.
[22]R. Balian and E. Brezin, Nuovo Cimento **LXIV B**, 37 (1969).
[23]P. Ring and P. Schuck, *The Nuclear Many-Body Problem* (Springer-Verlag, New York, 1980).
[24]N. Jacobson, *Lie Algebras* (Wiley, New York, 1962).
[25]The substitution of the momenta summation by an integration is correct in the thermodynamic ($\mathcal{N}\to\infty$) limit, provided the integrand $F(k)$ is finite for all k. In the case of long-range magnetic order, special care has to be taken of "Bose condensates" at $k = k^{bc}$ where $F(k^{bc}) \propto \mathcal{N}$.